

457 **A Additional Results**

458 In addition to the aggregated results in the main paper, we also provide per-task results for all  
 459 experiments and tasks in simulation. Our benchmark results are shown in Figure 7, and task transfer  
 460 results are shown in Figure 10. Per-task results for all of our ablations are shown in Figure 8 and  
 461 Figure 9.

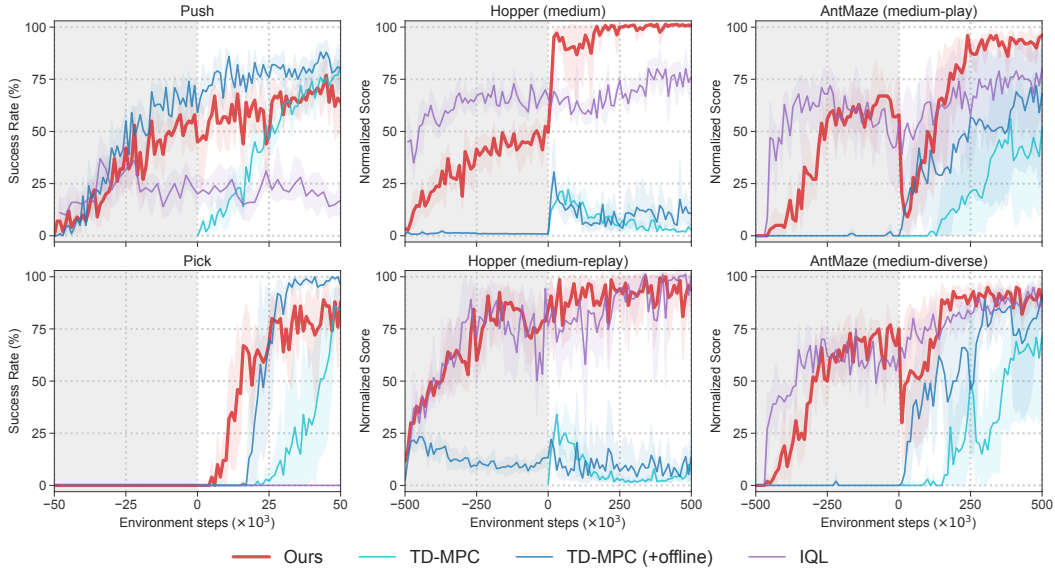


Figure 7. Comparison of our method against baselines. Offline pretraining is shaded gray. Mean of 5 seeds; shaded area indicates 95% CIs.

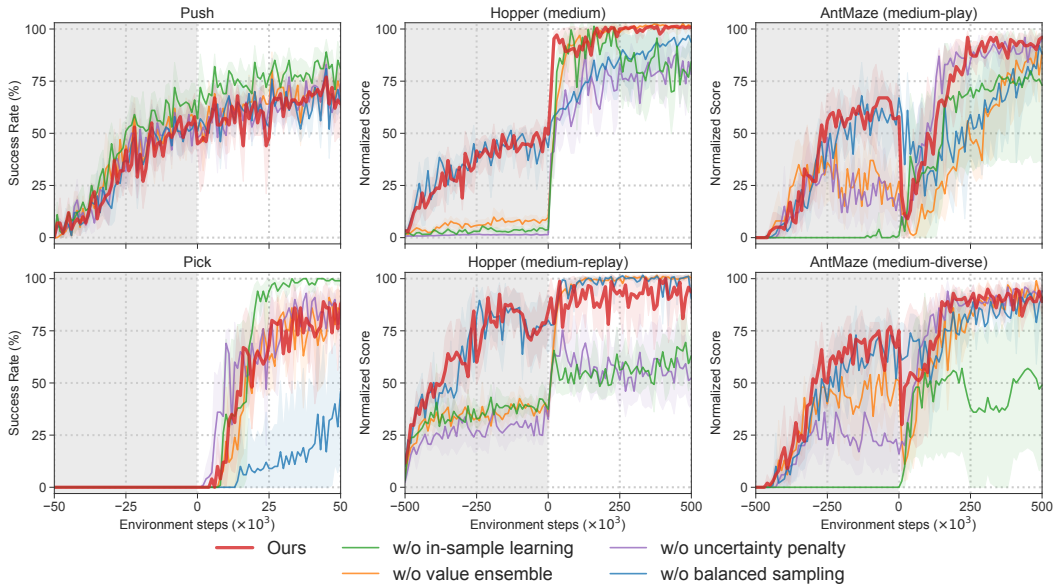


Figure 8. Ablation results on all tasks. Offline pretraining is shaded gray. Mean of 5 seeds; shaded area indicates 95% CIs.

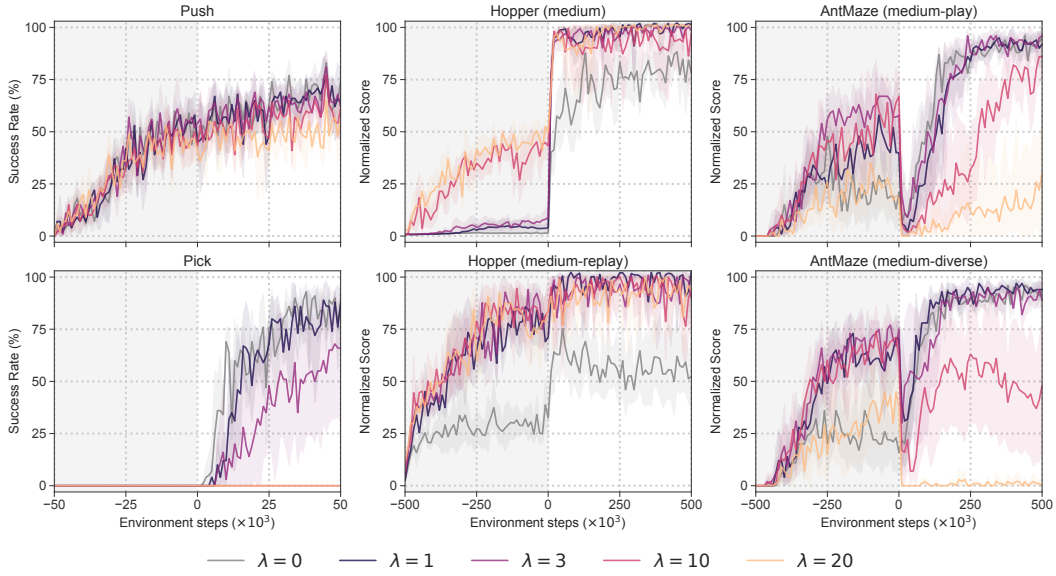


Figure 9. Ablation study on uncertainty coefficient ( $\lambda$ ). Offline pretraining is shaded gray. Mean of 5 seeds; shaded area indicates 95% CIs.

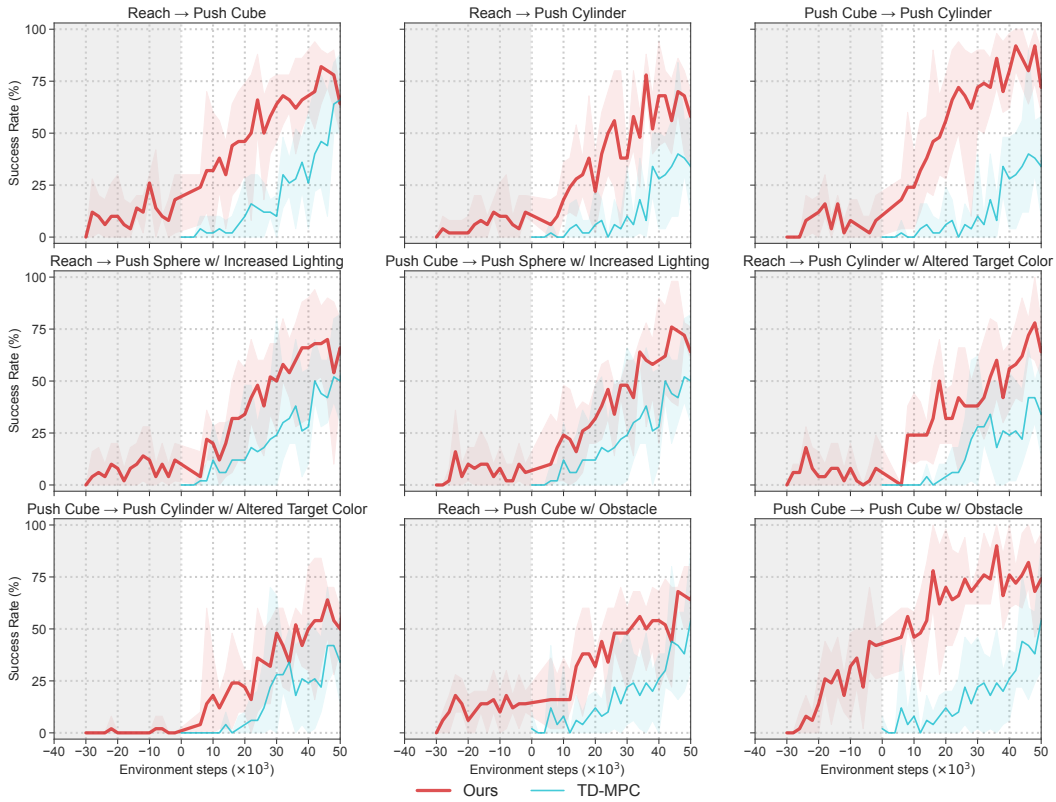


Figure 10. Task transfer results. Success rate (%) of our method and TD-MPC trained from scratch on all 9 simulated transfer tasks. We designed these tasks based on the xArm [27] task suite. Offline pretraining is shaded gray. Mean of 5 seeds; shaded area indicates 95% CIs.

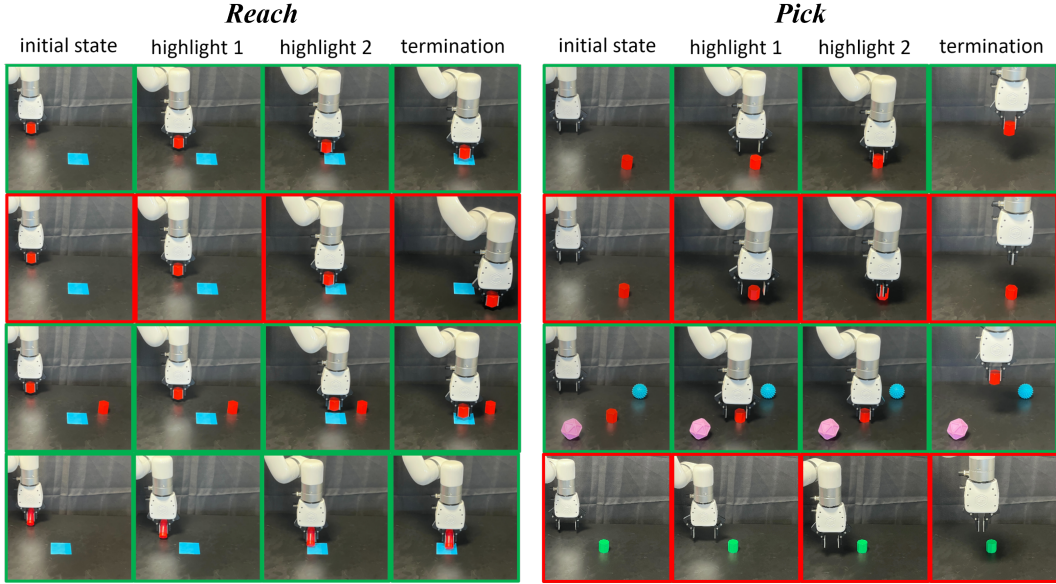


Figure 11. **Sample trajectories.** We include eight trajectories from the offline dataset or evaluation results, which illustrate all real-world tasks considered in this work. Successful trajectories are marked green while failed trajectories are marked red.

## 462 B Tasks and Datasets

### 463 B.1 Real-World Tasks and Datasets

464 We implement two visuo-motor control tasks, *reach* and  
 465 *pick* on a UFactory xArm 7 robot arm with an Intel Re-  
 466 alSense Depth Camera D435 as the only external sensor.  
 467 The observation space contains a  $224 \times 224$  RGB im-  
 468 age and an 8-dimensional robot proprioceptive state in-  
 469 cluding the position, rotation, and the opening of the end-  
 470 effector and a boolean value indicating whether the grip-  
 471 per is stuck. Both tasks are illustrated in Figure 3 (*second*  
 472 *from the left*). For safety reasons, we limit the moving  
 473 range of the gripper in a  $30\text{cm} \times 30\text{cm} \times 30\text{cm}$  cube, of  
 474 which projection on the table is illustrated in Figure 12.  
 475 To promote consistency between experiments, we evalu-  
 476 ate agents on a set of fixed positions, visualized as red  
 477 crosses in the aforementioned figure.

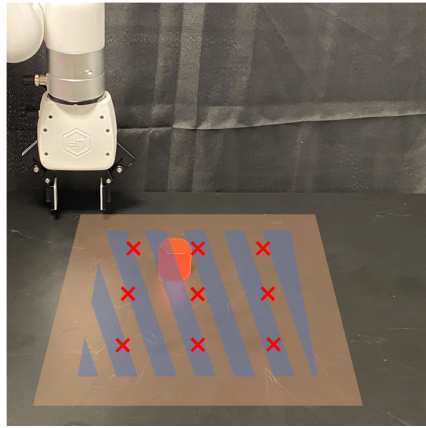


Figure 12. **Real-world workspace.** Moving range of the end-effector and the initialization range of target/object are shaded in the image. The positions for evaluation are labeled by crosses.

478 **Reach** The objective of this task is to accurately position the red hexagonal prism, held by the  
 479 gripper, above the blue square target. The action space of this task is defined by the first two dimen-  
 480 sions, which correspond to the horizontal plane. The agent will receive a reward of 1 when the object is  
 481 successfully placed above the target, and a reward of 0 otherwise. The offline dataset for *reach*  
 482 comprises 100 trajectories collected using a behavior-cloning policy, which exhibits an approximate  
 483 success rate of 50%. Additionally, there are 20 trajectories collected through teleoperation, where  
 484 the agent moves randomly, including attempts to cross the boundaries of the allowable end-effector  
 485 movement. These 20 trajectories are considered to be diverse and are utilized for conducting an  
 486 ablation study around the quality of the offline dataset.

487 **Pick** The objective of this task is to grasp and lift a red hexagonal prism by the gripper. The action  
 488 space of this task contains the position of the end-effector and the opening of the gripper. The agent

489 will receive a reward of 1 when the object is successfully lifted above a height threshold, a reward  
 490 of 0.5 when the object is grasped but not lifted, and a reward of 0 otherwise. The offline dataset for  
 491 *pick* comprises 200 trajectories collected using a BC policy that has an approximate success rate of  
 492 50%. Figure 11 shows sample trajectories from our offline dataset for *pick*.

493 **Real-world transfer tasks** We designed two transfer tasks for both *reach* and *pick*, as shown in  
 494 Figure 3 (the second from right). As the red hexagonal prism is an important indicator of the end-  
 495 effector position in *reach*, we modify the task by (1) placing an additional red hexagonal prism on  
 496 the table, alongside the existing one, and (2) replacing the object with a small red ketchup bottle,  
 497 whose bottom is not aligned with the end-effector. In *pick*, the red hexagonal prism is regarded as a  
 498 target object. Therefore we (1) add two distractors, each with a distinct shape and color compared  
 499 to the target object, and (2) change the color and shape of the object (from a red hexagonal prism  
 500 to a green octagonal prism). We’ve shown by experiments that different modifications will have  
 501 different effects on subsequent performance in finetuning, which demonstrates both the effectiveness  
 502 and limitation of the offline-to-online pipeline we discussed.

## 503 B.2 Simulation Tasks and Datasets

504 **xArm** *Push* and *pick* are two visuo-motor control tasks in the xArm robot simulation environ-  
 505 ment [27] implemented in MuJoCo. The observations consist of an  $84 \times 84$  RGB image and a  
 506 4-dimensional robot proprioceptive state including the position of the end-effector and the opening  
 507 of the gripper. The action space is the control signal for this 4-dimensional robot state. The tasks  
 508 are visualized in Figure 3 (left). *push* requires the robot to push a green cube to the red target. The  
 509 goal in *pick* is to pick up a cube and lift it above a height threshold. Handcrafted dense rewards are  
 510 used for these two tasks. We collected the offline data for offline-to-online finetuning experiments  
 511 by training TD-MPC agents from scratch on these tasks. We saved the first 40k environment steps  
 512 (800 trajectories) in the replay buffer as an offline dataset for each task. Figure 13 gives an overview  
 513 of the offline data distribution for the two tasks.

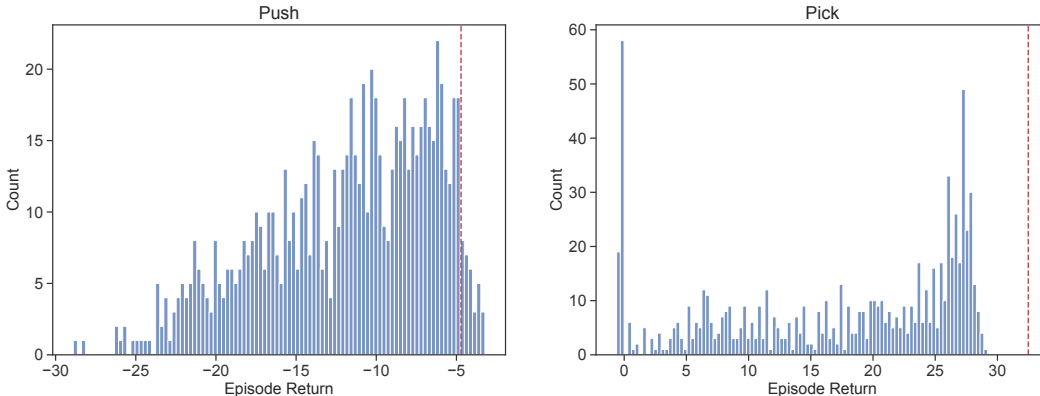
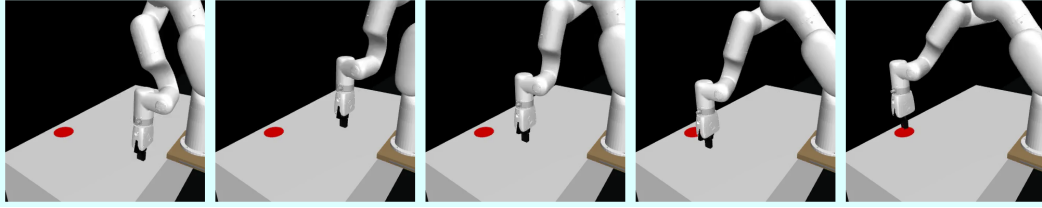
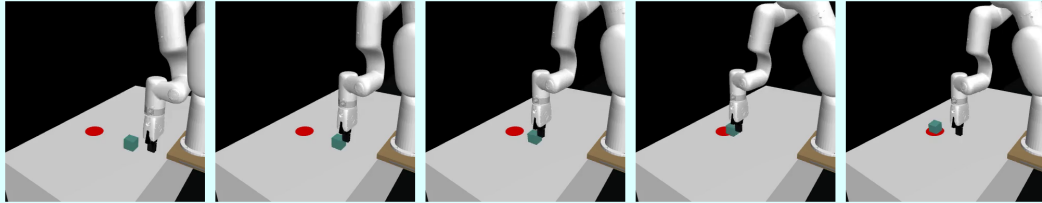


Figure 13. **Offline dataset statistics for xArm tasks in simulation.** We plot the distribution of episode returns for trajectories in the two offline datasets. The red line indicates the mean performance achieved by our method after online finetuning.

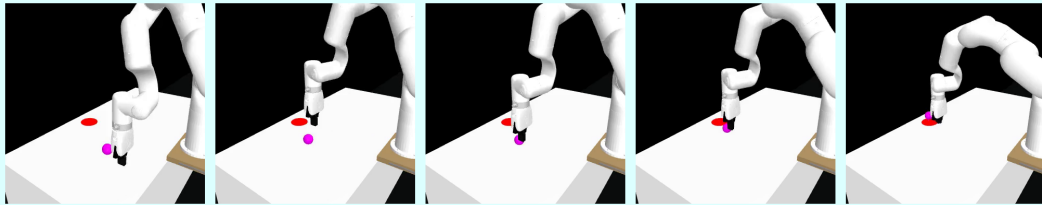
514 **Transfer tasks** We designed nine transfer tasks based on *reach* (the same task as real *reach* but  
 515 simplified because of the knowledge of ground-truth positions) and *push* in simulation to evaluate  
 516 the generalization capability of offline pretrained model. Compared to real-world tasks, the online  
 517 budget is abundant in simulation, thus we increase the disparity between offline and online tasks such  
 518 as finetuning on a totally different task. As the target point for both tasks is a red circle, we directly  
 519 use *reach* as offline pretrain task and online finetuning on different instances of *push* including push  
 520 cube, push sphere, push cylinder, and push cube with an obstacle. All these tasks are illustrated in  
 521 Figure 14.



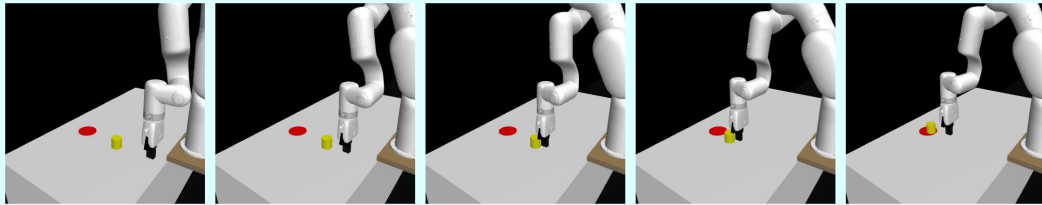
(a) Reach.



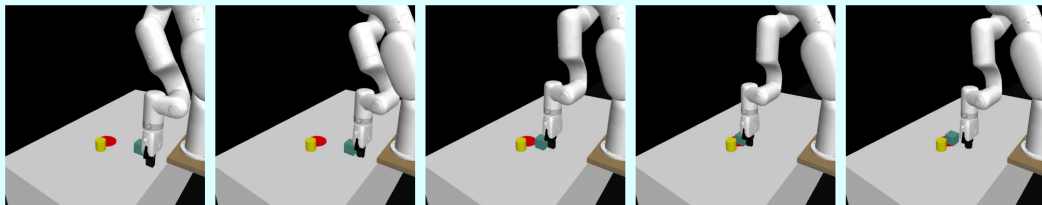
(b) Push.



(c) Push sphere with increased lighting.



(d) Push cylinder.



(e) Push with obstacle.

**Figure 14. Transfer tasks in our simulated xArm environments.** We consider a total of 9 transfer settings in simulation. We here visualize a trajectory for each of the tasks used in our xArm experiments. Task labels correspond to those shown in Figure 10.

522 **D4RL** We consider four representative tasks from two domains (Hopper and AntMaze) in the  
 523 D4RL [26] benchmark. Each domain contains two data compositions. *Hopper* is a Gym locomotion  
 524 domain where the goal is to make hops that move in the forward (right) direction. Observations  
 525 contain the positions and velocities of different body parts of the hopper. The action space is a 3-  
 526 dimension space controlling the torques applied on the three joints of the hopper. *Hopper (medium)*  
 527 uses 1M samples from a policy trained to approximately 1/3 the performance of the expert, while  
 528 *Hopper (medium-replay)* uses the replay buffer of a policy trained up to the performance of the

529 medium agent. *Antmaze* is a navigation domain with a complex 8-DoF quadruped robot. We use  
 530 the *medium* maze layout, which is shown in Figure 3 (left). The *play* dataset contains 1M samples  
 531 generated by commanding specific hand-picked goal locations from hand-picked initial positions,  
 532 and the *diverse* dataset contains 1M samples generated by commanding random goal locations in  
 533 the maze and navigating the ant to them. This domain is notoriously challenging because of the  
 534 need to “stitch” suboptimal trajectories. These four tasks are officially named *hopper-medium-v2*,  
 535 *hopper-medium-replay-v2*, *antmaze-medium-play-v2* and *antmaze-medium-diverse-v2*  
 536 in the D4RL benchmark.

## 537 C Implementation Details

538 ***Q*-ensemble and uncertainty estimation** We provide PyTorch-style pseudo-code for the imple-  
 539 mentation of the *Q*-ensemble and uncertainty estimation discussed in Section 3.2. Here *Qs* is a list  
 540 of *Q*-networks. We use the minimum value of two randomly selected *Q*-networks for *Q*-value es-  
 541 timation, and the uncertainty is estimated by the standard deviation of all *Q*-values. We use five  
 542 *Q*-networks in our implementation.

```
def Q_estimate(Qs, z, a):
    x = torch.cat([z, a], dim=-1) # concatenate (latent) state and action
    idxs = random_choice(len(Qs), 2, replace=False) # randomly select two distinct Qs
    q1, q2 = Qs[idxs[0]](x), Qs[idxs[1]](x)
    return torch.min(q1, q2) # return the minimum of the two as Q value estimation

def Q_uncertainty(Qs, z, a):
    x = torch.cat([z, a], dim=-1) # concatenate (latent) state and action
    qs = torch.stack(list(q(x) for q in Qs), dim=0)
    uncertainty = qs.std(dim=0) # compute the standard deviation as uncertainty
    return uncertainty
```

543 **Network architecture** For the real robot tasks and simulated xArm tasks where observations con-  
 544 tain both an RGB image and a robot proprioceptive state, we separately embed them into feature  
 545 vectors of the same dimensions with a convolutional neural network and a 2-layer MLP respectively,  
 546 and do element-wise addition to get a fused feature vector. For D4RL tasks where observations are  
 547 state features, only the state encoder is used. We use five *Q*-networks to implement the *Q*-ensemble  
 548 for uncertainty estimation. All *Q*-networks have the same architecture. An additional *V* network is  
 549 used for state value estimation as discussed in Section 3.1.

550 **Hyperparameters** We list the hyperparameters of our algorithm in Table 5. The hyperparameters  
 551 related to our key contributions are highlighted.

552 **Other details** We apply image shift augmentation [49] to image observations, and use Prioritized  
 553 Experience Replay (PER; [50]) when sampling from replay buffers.

## 554 D Baselines

555 **TD-MPC** We use the same architecture and hyperparameters for our method and our two  
 556 TD-MPC baselines as in the public TD-MPC implementation from [https://github.com/  
 557 nicklashansen/tdmpc](https://github.com/nicklashansen/tdmpc), except that we use two encoders, one for each modality, in the real robot  
 558 and xArm tasks that use both visual inputs and robot proprioceptive information. For the **TD-MPC**  
 559 **(+offline)** baseline, we naively pretrain the model on offline data and then finetune it with online RL  
 560 without any changes to hyperparameters.

561 **IQL** We use the official implementation from [https://github.com/ikostrikov/implicit\\_  
 562 q\\_learning](https://github.com/ikostrikov/implicit_q_learning) for the IQL baseline. We use the same hyperparameters that the authors used  
 563 for D4RL tasks. For xArm tasks, we perform a grid search over the hyperparameters  $\tau \in$

Table 5. Hyperparameters.

Hyperparameter	Value
Expectile ( $\tau$ )	0.9 (AntMaze, xArm) 0.7 (Hopper)
AWR temperature ( $\beta$ )	10.0 (AntMaze) 3.0 (Hopper, xArm)
Uncertainty coefficient ( $\lambda$ )	1 (xArm) 3 (AntMaze) 20 (Hopper)
$Q$ ensemble size	5
Batch size	256
Learning rate	3e-4
Optimizer	Adam( $\beta_1 = 0.9, \beta_2 = 0.999$ )
Discount	0.99 (D4RL) 0.9 (xArm)
Action repeat	1 (D4RL) 2 (xArm)
Value loss coefficient	0.1
Reward loss coefficient	0.5
Latent dynamics loss coefficient	20
Temporal coefficient	0.5
Target network update frequency	2
Polyak	0.99
MLP hidden size	512
Latent state dimension	50
Population size	512
Elite fraction	50
Policy fraction	0.1
Planning iterations	6 (xArm) 1 (D4RL)
Planning horizon	5
Planning temperature	0.5
Planning momentum coefficient	0.1

564  $\{0.5, 0.6, 0.7, 0.8, 0.9, 0.95\}$  and  $\beta \in \{0.5, 1.0, 3.0, 10.0\}$ , and we find that expectile  $\tau = 0.95$   
565 and temperature  $\beta = 10.0$  achieves the best results. We add the same image encoder as ours to the  
566 IQL implementation in visuo-motor control tasks.